

## Article

# Dynamic Prediction of Air Traffic Situation in Large-Scale Airspace

Dong Sui, Kechen Liu \*  and Qian Li

College of Civil Aviation, Nanjing University of Aeronautics and Astronautics, Nanjing 210016, China

\* Correspondence: liukechen@nuaa.edu.cn

**Abstract:** Air traffic situation prediction is critical for traffic flow management and the optimal allocation of airspace resources. In this study, the multi-sector airspace scenario is abstracted into an undirected graph. A spatiotemporal graph convolutional network (STGCN) model is developed to portray the spatiotemporal correlation between the sector operational situation changes. The model can predict multi-sector operational situations using time series data such as sector operational situation data and traffic volume within the sector. Experimenting on the air traffic situation dataset of 30 area sectors in the Shanghai control area revealed that the STGCN model has a prediction accuracy of above 90%, and it outperforms the benchmark method of traditional traffic prediction. This proves the effectiveness of the proposed situation prediction model.

**Keywords:** graph convolutional network; gated recurrent unit; airspace air traffic situation prediction; spatiotemporal correlation



**Citation:** Sui, D.; Liu, K.; Li, Q. Dynamic Prediction of Air Traffic Situation in Large-Scale Airspace. *Aerospace* **2022**, *9*, 568. <https://doi.org/10.3390/aerospace9100568>

Academic Editor: Álvaro Rodríguez-Sanz

Received: 13 August 2022

Accepted: 26 September 2022

Published: 29 September 2022

**Publisher's Note:** MDPI stays neutral with regard to jurisdictional claims in published maps and institutional affiliations.



**Copyright:** © 2022 by the authors. Licensee MDPI, Basel, Switzerland. This article is an open access article distributed under the terms and conditions of the Creative Commons Attribution (CC BY) license (<https://creativecommons.org/licenses/by/4.0/>).

## 1. Introduction

As flight traffic continues to increase, the traditional air traffic management methods can no longer meet the current practical needs. Air traffic situation prediction can help air traffic management departments anticipate the trend of future operation status to identify congested airspace and formulate traffic balancing and management measures in advance. Large-scale controlled airspace is usually divided into multiple controlled sectors. In the actual operation process, the operation statuses of neighboring sectors are interrelated and affect each other. If the traffic situation of each sector is predicted separately, the coupling relationship between the sectors is ignored. Therefore, the traffic situation prediction problem in large-scale airspace needs to consider the correlation between sectors.

Air traffic situation assessment is an objective representation of the airspace operational status, and its results are also the basis for air traffic situation prediction. The mainstream assessment methods mainly represent the air traffic situation with the help of the concept of air traffic complexity (also called airspace complexity or air traffic control complexity) [1–3]. Since there is no precise definition of this concept and many factors affect air traffic complexity, researchers can deconstruct air traffic complexity to represent air traffic situations from multiple perspectives [4–6].

Air traffic complexity evaluation studies can be broadly divided into two categories, and their representative studies are shown in Table 1. The first type of research evaluates air traffic complexity by analyzing the operation process from a single evaluation perspective, such as the number of potential flight conflicts and flight trajectory disorderliness. The analytical formula can directly calculate complexity index. However, it is challenging to represent the overall complexity of air traffic comprehensively because it only focuses on one critical process or complex situation in the air traffic operation process. Another type of study designs and selects multiple indicators affecting air traffic complexity from multiple perspectives and tries to build an air traffic complexity evaluation index system based on the concept of dynamic density. Linear regression and machine learning methods

establish the mapping relationship between the indicators and the posture. However, currently, the sample set is often obtained using controllers' manual scoring, so the cost of obtaining labeled samples is high. Moreover, a controller is often responsible for only one specific sector, so only samples from that specific sector can be evaluated, which leads to the fact that models trained using data from specific sectors can only be used on the specific sectors involved in the training. The evaluation methods of semi-supervised learning and migration learning require only a small number of labeled samples to train the model. However, the labeled samples are challenging to apply to other sectors. The unsupervised clustering approach does not require labeled samples but still requires air traffic controllers to evaluate the model's accuracy.

**Table 1.** Representative studies of air traffic complexity.

Research Type	Researchers	Assessment Perspectives and Indicators	Assessment Methodology
Single Perspective	K. Lee [2]	Analysis of traffic complexity based on aircraft disturbance effects	Representation of airspace complexity as a complexity diagram
	M. Prandini [7]	Conflict risk estimation of flight trajectories	Compute the analytic approximation of the complexity measure for each point in the airspace
	D. Delahaye [1,5,8]	Trajectory disorder metric based on Lyapunov exponent	Representation of airspace complexity as a complexity diagram
Multi-Perspective	I.V. Laudeman [4]	The dynamic density model was constructed by selecting eight indicators, including the number of aircrafts, the number of conflicts, and the number of course changes	Linear regression method
	D. Gianazza [6,9,10]	Considering two dimensions of airspace structure and traffic characteristics, a total of 28 indicators were selected	BP neural network model
	M. Xiao [11]	Based on the original evaluation indicators constructed by D. Gianazza, seven key indicators were selected from them for the experiment	BP neural network model
	X. Zhu [12]	Complexity evaluation refers to the evaluation index system constructed by M. Xiao	Semi-supervised learning methods
	X. Cao [13]	The evaluation system constructed by D. Gianazza was chosen for the complexity evaluation	Transfer learning methods
	Z. Zhang [14]	Based on the original evaluation index system constructed by D. Gianazza	Unsupervised clustering methods

For the problem of air traffic situation assessment, no standardized assessment method has been formed yet. The reasons are mainly in two aspects: different scholars have constructed various air traffic complexity evaluation index systems, but a recognized evaluation system has not been formed; using machine learning methods to evaluate the air traffic situation, the calibration process, and the validation process of control experts for large sample sizes are costly, and it is not easy to eliminate the subjective influence of control experts. Since the air traffic situation samples in different sectors are not universal, the air traffic situation assessment process with controllers' participation also limits the assessment model's use, which does not apply to the situation assessment process in other sectors and large-scale airspace. Therefore, a more concise and objective way to evaluate the traffic situation in large-scale airspace would be to eliminate the subjectivity and improve the applicability and accuracy of the air traffic situation assessment model.

Unlike the method of using sector operation status data (sector merging and splitting operation information) to classify the operation of airspace into three states [10], this paper fully applies the flight operation data and flow control information released by the air traffic management department to define three types of sector operation states: free state, saturation state, and intermediate state. Flow control information advises the restriction of subsequent flight operations, issued by the controller after applying to the air traffic flow management department voluntarily when their workload is too high; consequently, it can reflect the controller's workload more accurately than the sector operation status data, and there is no data distortion. Compared with calculating indicators to assess the air traffic situation, the flow control data represents the controller's judgment of the air traffic situation, so there is no need for further verification by control experts. In sample acquisition, the method only needs to obtain the flow control and flight flow data from the air traffic management department for the target area and target time range to calibrate many samples. The sample acquisition process is fast and straightforward.

Most of the research on air traffic situations has focused on how to measure it, while few studies have focused on the problem of predicting air traffic situations. Related studies are also mainly focused on predicting traffic flow and the indicators related to air traffic situations [15,16]. In the actual operation process, the operational status of neighboring sectors is often interrelated due to the connection of the route network between sectors. If we only focus on the individual sector's situation, the interaction effect between sectors will be ignored. The situation prediction results are difficult to apply to actual air traffic management. Therefore, the interaction between sectors cannot be neglected when predicting the traffic situation in large-scale airspace.

In recent years, spatiotemporal prediction models constructed using graphical convolutional networks (GCN) and recurrent neural networks (RNN) have become a research hotspot in traffic prediction. The related literature is summarized in Table 2. Among them, different studies have also been introduced in the modeling process, such as the attention mechanism [17,18], the sequence-to-sequence (Seq2Seq) model [19] and the Transformer model [20]. The modeling approach of combining recurrent neural networks with GCN can predict the sectoral situation in the time dimension. More importantly, it can integrate the interaction effects between sectors in the spatial dimension, so this paper uses the modeling framework of graphical convolutional networks combined with RNN to study large-scale airspace operational situation prediction.

**Table 2.** Summary of spatiotemporal prediction modeling methods.

Number	Model	Year	Spatial Dimension	Time Dimension	External Influences
1	A3T-GCN [17]	2020	GCN	GRU + Attention	—
2	ASTGCN [18]	2019	GCN + Attention	CNN + Attention	—
3	DCRNN [19]	2018	GCN	GRU + Seq2Seq	—
4	STGNN [20]	2020	GCN	GRU + Transformer	—
5	T-GCN [21]	2019	GCN	GRU	—
6	AST-GCN [22]	2021	GCN	GRU	POIs, Weather
7	AGCRN [23]	2020	GCN	GRU	—
8	DGCRN [24]	2021	GCN	GRU + Seq2Seq	—
9	ST-GCN [25]	2018	GCN	CNN	—
10	Graph-WaveNet [26]	2019	GCN	CNN	—
11	STSGCN [27]	2020	GCN	GCN	—
12	STFGNN [28]	2021	GCN	CNN	—

In this paper, by utilizing the ability of a graph neural network to analyze graph data, the sectors are abstracted as nodes, the spatial connections between sectors are edges, and multiple sectors are represented as undirected graphs. The spatial correlation between airspace sectors is learned using GCN modeling and combined with an RNN to predict the future airspace operational situation.

The objective of this paper is to make full use of the traffic control data and sector traffic data to complete the rapid calibration of the air traffic situation and use the spatiotemporal graph convolutional network (STGCN) model to realize the situation prediction in large-scale airspace. This will provide auxiliary decision-making information for air traffic management departments when formulating traffic management strategies and implementing traffic management measures.

This study makes the following novel contributions to the literature:

1. A type of operational data that more accurately reflects the controller's workload, i.e., flow control data, was used to accomplish a rapid calibration of air traffic situations.
2. Considering the spatial and temporal correlation between sectors, the scope of the study is not limited to a single sector. A large-scale airspace operational situation prediction model is established based on the GCN. The prediction results can reflect the characteristics of the changes in the operational status of large-scale airspace, which can provide a decision basis for optimizing the traffic flow and sector resource allocation.

The rest of the paper is organized as follows: Section 2 describes the problem of assessing and predicting the traffic situation in large-scale airspace. Section 3 describes the framework and construction process of the STGCN model. Section 4 presents the experimental dataset of the model, parameter settings, and experimental results. Section 5 concludes the paper.

## 2. Air Traffic Situation Assessment and Prediction

### 2.1. Air Traffic Situational Assessment Method

Air traffic situations can be understood as the operational status in a specific airspace environment (sector structure and meteorological conditions). Different scholars have proposed various methods to characterize the airspace operational situation [1,4,6]. As mentioned above, for large-scale airspace, an objective and concise way must be designed to solve the air traffic situation assessment problem, while avoiding the construction of a complicated air traffic complexity evaluation index system and the sample calibration process by air traffic control experts.

This paper uses flow control information combined with flight flow information to determine the operational status of a sector. Flow control information is a kind of instruction issued by air traffic management to restrict flight flow at a specific time and in a particular area. It is only given when controllers are overloaded with work or encounter specific circumstances so that it can indicate the operational status of the restricted airspace. The spatial and temporal accuracy of the flow control information also provides the conditions to count the operating situation of the airspace under a specific period.

In this study, we use the sector operational saturation degree to characterize the operational status and define three airspace operational states: free state, saturation state, and intermediate state based on the real traffic statistics and flow control information, as shown in Figure 1. When high traffic volume or bad weather causes an excessive controller load, the air traffic control department issues flow control instructions to ensure operational safety. In this study, we consider the operational state of the sector during the flow control period as a saturation state with a saturation degree of 100%.

The free state is defined as the operational state of the sector during the hours of extremely low traffic. According to the sector hourly flight volume statistics, as shown in Figure 2, the flight volume is the lowest from 00:00 to 06:00 daily. Thus, the sector is defined to be in a free state from 00:00 to 06:00 daily. Due to the low number of flights in the free state, the operating pressure is low. The sector saturation value is set to 0 in this state. The intermediate state is the operational state other than the free state and saturation state with a saturation degree value between 0 and 100%.

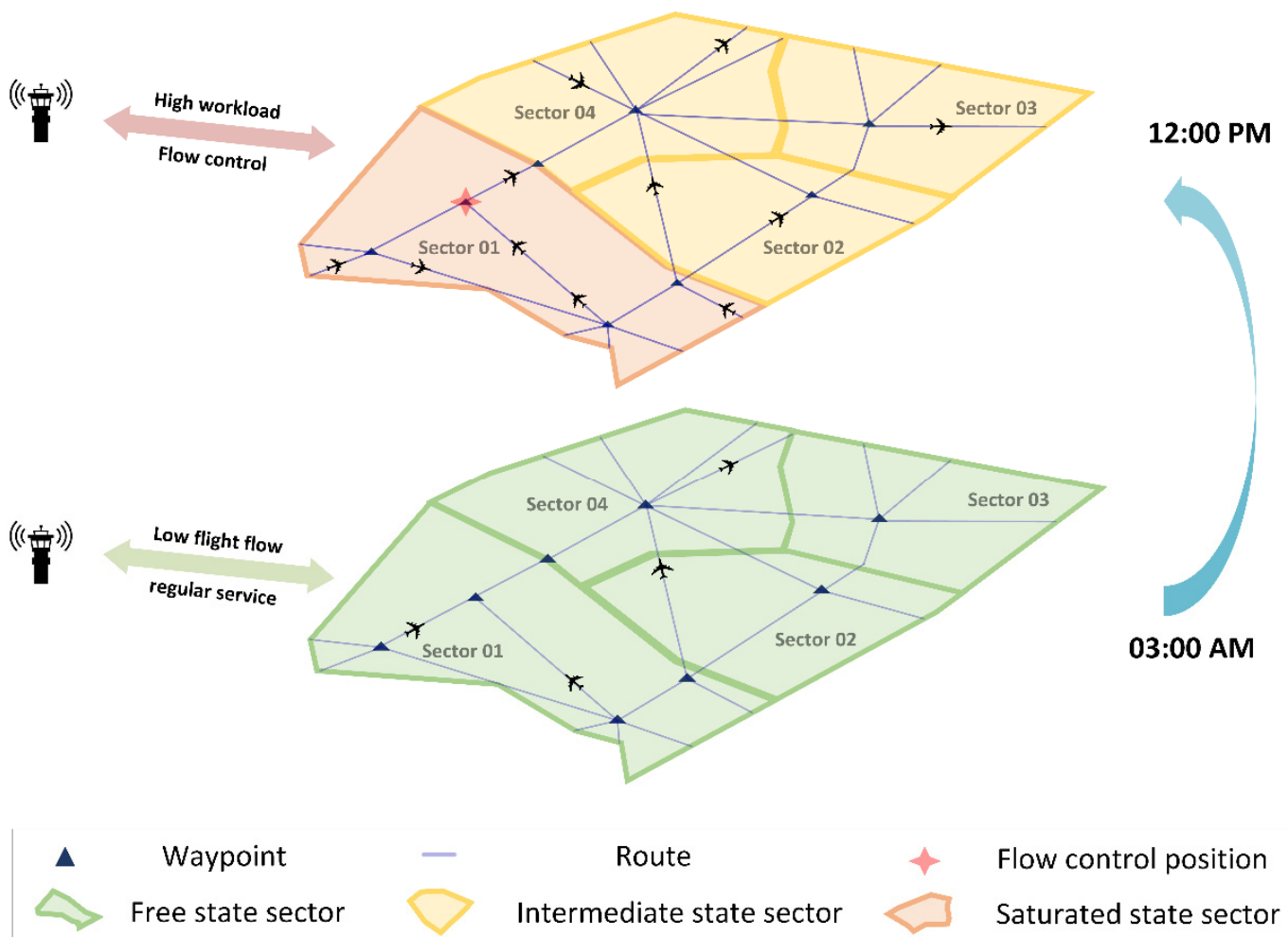


**Figure 1.** The air traffic situation of the four control sectors in the Shanghai control area at different times.

In this paper, the state labels of free state, intermediate state and saturated state are represented by three rank values of 1, 2, and 3, respectively. Considering that the three predicted statuses are ordered variables with a size relationship, the loss value calculation is not accurate enough when the prediction accuracy is directly measured by the classification method. Therefore, this paper takes the state labels (1, 2, and 3) set for a free state, intermediate state, and saturated state as anchor points and measures the prediction accuracy by regression prediction, after which the nearest state anchor point is selected as its final air traffic situation prediction result, according to the prediction value of the sample.

## 2.2. Air Traffic Situation Prediction Problem

In order to reasonably allocate the workload of air traffic controllers, the airspace is divided into sectors according to the distribution of routes and waypoints, and each sector is assigned its corresponding controller to ensure operational safety. Sectors are the fundamental units of airspace operation, and the coordinated operation of multiple sectors results in seamless air traffic service. To represent the interrelations between sectors, this study abstracts the controlled airspace as an undirected graph with sectors as nodes  $v$  and the connection relationship between sectors as edges  $e$ . Taking Figure 1 as an example, the four sectors in the graph are abstracted as nodes. The existence of an airway connection between sectors determines whether or not the sectors are connected by edges. Finally, as

shown in Figure 3, the undirected graph  $G$  with four nodes ( $v_1, v_2, v_3, v_4$ ) and five edges ( $e_1, e_2, e_3, e_4, e_5$ ) is obtained.

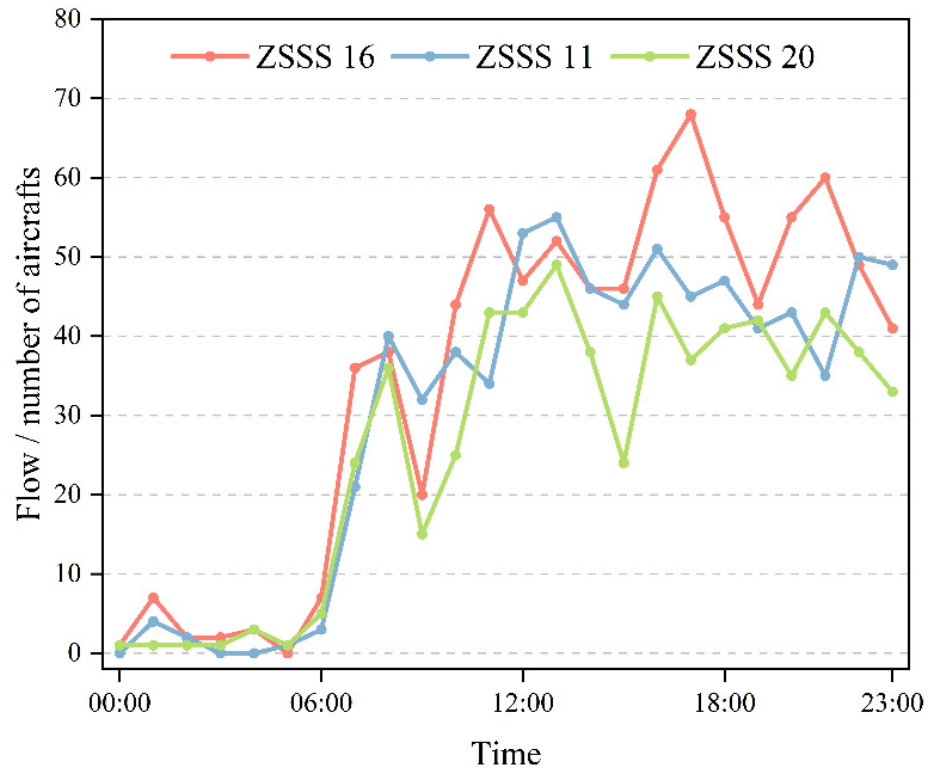


**Figure 2.** 24-h traffic statistics for control sectors 16, 11, and 20 in the Shanghai control area. Statistics based on flight trajectory data on 6 August 2018.

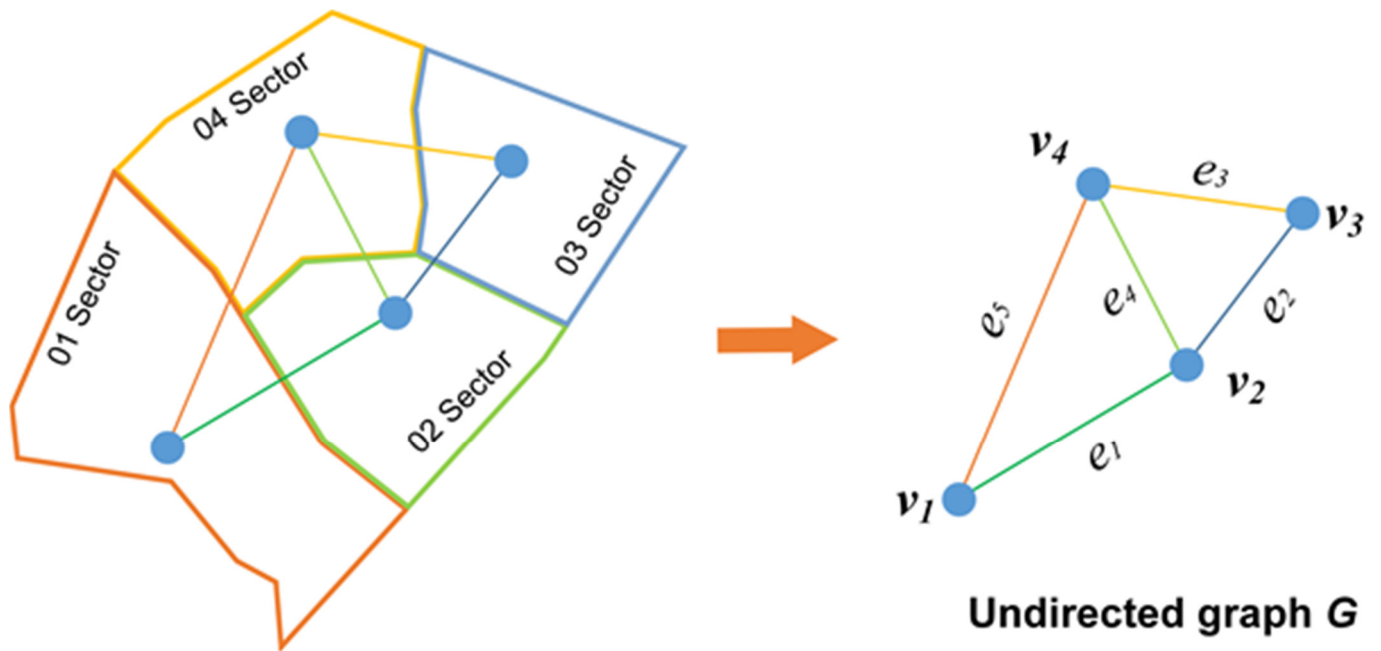


**Figure 3.** Abstraction to undirected graph based on sector adjacency. Representation of multiple sectors as undirected graphs based on the route connection relationship between sectors.

Multi-sector airspace operational situation prediction aims to predict the operational situation in future periods based on the air traffic situation in past periods. The traditional

time series forecasting method can only predict the trend of the operational situation from the time dimension; however, it cannot analyze the interrelation between sectors from the spatial dimension. In this study, the airspace network is first abstracted into the form of an undirected graph for analysis. As shown in Figure 3, the undirected graph  $G$  is an irregular graph data structure that does not apply to the traditional convolutional neural network model. GCN can handle graph data in non-Euclidean space and is currently beneficial in predicting road traffic parameter issues [21,22,29,30]. Thus, we use the GCN for modeling.

The prediction process is based on the time series data  $X \in \mathbb{R}^{n \times t}$  generated by air traffic situation features, where  $n$  denotes the number of nodes and  $t$  denotes the number of time slices. The spatial features among the nodes are first studied using a graphical convolutional network, which is further combined with an RNN for the long-term prediction of air traffic situations. The goal of multi-sector operational situation prediction is to develop a function  $f(\bullet)$  capable of mapping the situation characteristics of the past  $T'$  time slices to those of the future  $T$  time slices. For a given airspace network graph  $G$ , the situation prediction problem can be represented by Equation (1).

$$[X^{(t-T'+1)}, \dots, X^{(t)}; G] \xrightarrow{f(\bullet)} [X^{(t+1)}, \dots, X^{(t+T')}] \tag{1}$$

### 3. Air Traffic Situation Prediction Model Based on GCN

STGCN, a combination of GCN and RNN, is established to study the spatiotemporal correlation between the nodes on the graph by considering the spatiotemporal situation characteristics of each sector in the past as the input of the prediction model. The overall model framework is shown in Figure 4, which primarily consists of three parts: the input module, the spatiotemporal prediction module, and the output module.

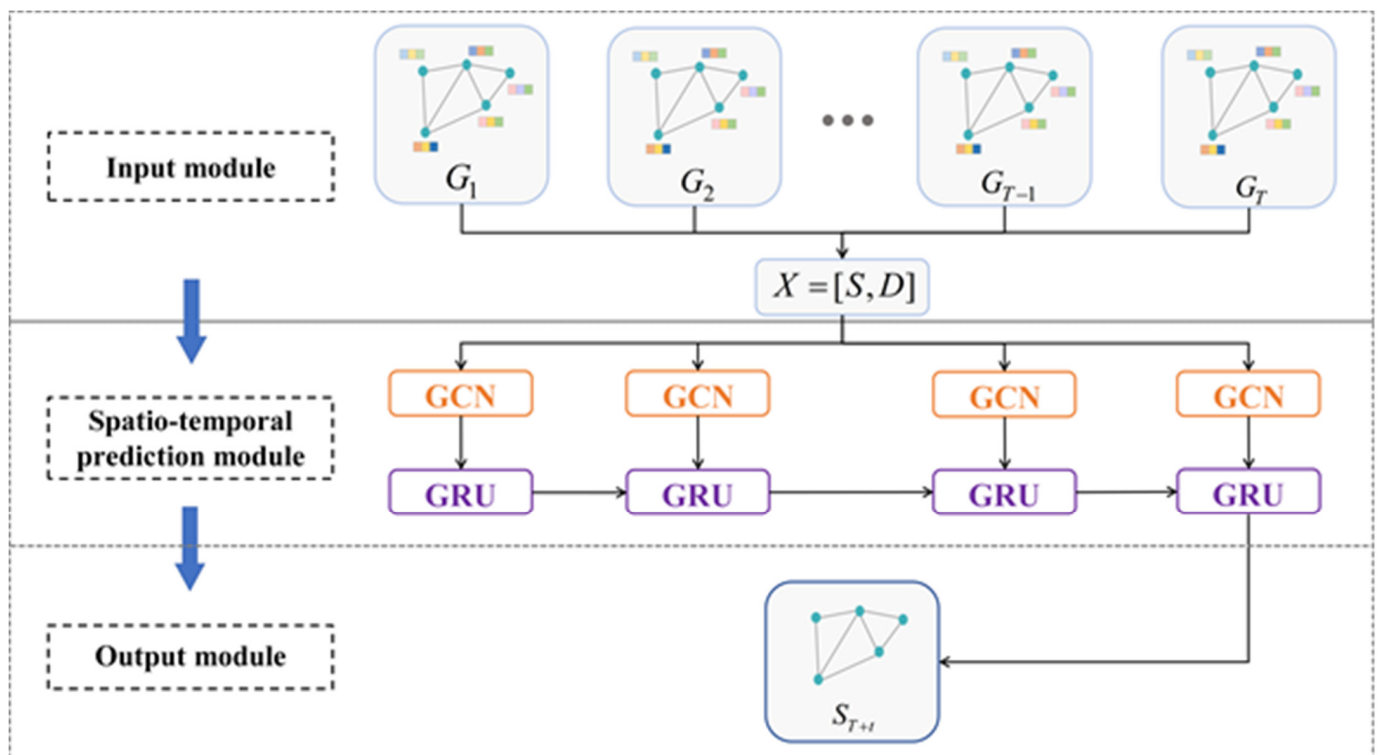


Figure 4. STGCN model framework.

The traffic volume, the most intuitive dynamic influencing factor, is closely related to changes in the air traffic situation. The higher the traffic volume, the more frequently the aircraft status changes, and the more complex the operational situation becomes. In this

study, real-time traffic volume is used as the dynamic feature and air traffic situation data are integrated as the model input.

The airspace is divided into  $n$  sectors. The situation feature matrix is  $s \in R^{n \times t}$ , and the traffic volume matrix is  $D \in R^{n \times t}$  in time period  $1 \sim t$ . The new feature matrix  $X = [S, D]$  is obtained by merging  $S$  and  $D$  as the model input. The feature matrix is merged as shown in Equation (2). The final input of the model is  $X \in R^{n \times 2t}$ .

$$\begin{bmatrix} x_{11} & x_{12} & x_{13} & \cdots & x_{1t} \\ x_{21} & x_{22} & x_{23} & \cdots & x_{2t} \\ x_{31} & x_{32} & x_{33} & \cdots & x_{3t} \\ \vdots & \vdots & \vdots & \ddots & \vdots \\ x_{n1} & x_{n2} & x_{n3} & \cdots & x_{nt} \end{bmatrix} = \begin{bmatrix} s_{11} & s_{12} & s_{13} & \cdots & s_{1t}d_{11} & d_{12} & d_{13} & \cdots & d_{1t} \\ s_{21} & s_{22} & s_{23} & \cdots & s_{2t}d_{21} & d_{22} & d_{23} & \cdots & d_{2t} \\ s_{31} & s_{32} & s_{33} & \cdots & s_{3t}d_{31} & d_{32} & d_{33} & \cdots & d_{3t} \\ \vdots & \vdots & \vdots & \ddots & \vdots & \vdots & \vdots & \ddots & \vdots \\ s_{n1} & s_{n2} & s_{n3} & \cdots & s_{nt}d_{n1} & d_{n2} & d_{n3} & \cdots & d_{nt} \end{bmatrix} \quad (2)$$

The spatiotemporal prediction module combines GCNs and gated recurrent units (GRUs) to model and analyze the spatiotemporal correlation between sectors. The spatial structure characteristics of the sectors are understood based on GCN, which is based on the graph Fourier transform and the convolution theorem, first converting the data from the spatial domain to the spectral domain for processing, and then back to the spatial domain after processing.

Assume that the airspace has  $n$  sectors, and the node feature matrix is  $X$ . Considering the airspace operational situation feature  $x \in R^n$  at time  $t$  as the graph signal, the convolution of  $x$  with filter  $g$  on the spectral domain is defined as shown in Equation (3) according to the convolution theorem:

$$x * g = U(U^T x \odot U^T g) = U g_\theta U^T x \quad (3)$$

where  $g_\theta$  is the parameterizable convolution kernel.  $U$  is the Fourier basis obtained by performing an eigenvalue decomposition  $L = U\Lambda U^T$  of the Laplacian matrix  $L$  of the graph.  $\Lambda = \text{diag}([\lambda_0, \dots, \lambda_{N-1}]) \in R^{n \times n}$  is the diagonal matrix composed of the eigenvalues of  $L$ . In spectral graph theory, the graph structure is represented by  $L$  with the formula  $L = D - A$ , where  $D$  is the degree matrix and  $A$  is the adjacency matrix. The features of the graph structure are extracted by performing an eigenvalue decomposition of  $L$ . The convolution of each layer of the graph in the GCN can be defined as Equation (4):

$$H^{l+1} = f(H^l, A) = \sigma(\hat{A}H^lW^l) \quad (4)$$

where  $H^l$  denotes the node vector of layer  $l$  and  $W^l$  denotes the parameters of the corresponding layer.  $\hat{A} = \tilde{D}^{-\frac{1}{2}}\tilde{A}\tilde{D}^{-\frac{1}{2}}$ ,  $\tilde{A} = A + I_N$ , and  $\tilde{D}_{ii} = \sum_j \tilde{A}_{ij}$ . In this study, a two-layer GCN is designed to study the spatial structural features between sectors in the airspace, and the model expression is given in Equation (5). The model structure is shown in Figure 5. The adjacency matrix  $A$  and the merged feature matrix  $X$  are used as model inputs. ReLU is used as the activation function to study the new airspace operational situation features, denoted as  $Z = \hat{A}\text{ReLU}(\hat{A}XW^0)W^1$ .

$$f(X, A) = \sigma(\hat{A}\text{ReLU}(\hat{A}XW^0)W^1) \quad (5)$$

Using  $Z$  as the input, GRU for time-dependent modeling sets two gate functions: the update gate  $u_t$  and the reset gate  $r_t$ . The network structure is shown in Figure 6. Due to the gating mechanism, GRU retains the changing trend of historical situation information when predicting air traffic situations and studies the dynamic time-varying characteristics from the situation data. GRU predicts the future air traffic situation taking the airspace operational situation characteristics  $z_t$  of the current moment and the hidden state of the previous moment  $h_{t-1}$  as the input  $h_t$ .  $\tilde{h}_t$  is the candidate state of the current moment. The state update of the GRU network is shown in Equations (6)–(9). The whole spatiotemporal prediction process is shown in Figure 4.

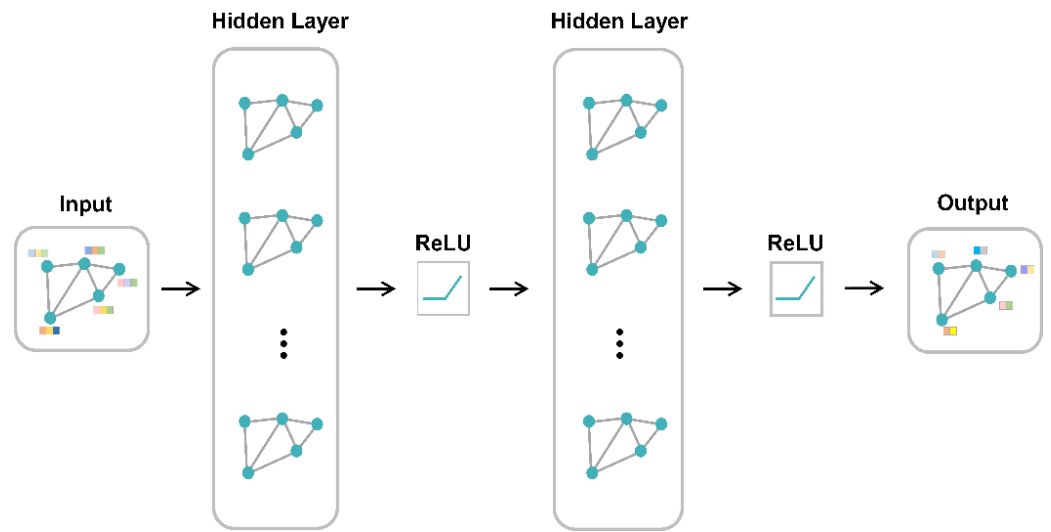


Figure 5. GCN model framework.

$$u_t = \sigma(W_u z_t + U_u h_{t-1} + b_u) \tag{6}$$

$$\tilde{h}_t = \tanh(W_h z_t + U_h (r_t \odot h_{t-1}) + b_h) \tag{7}$$

$$r_t = \sigma(W_r z_t + U_r h_{t-1} + b_r) \tag{8}$$

$$h_t = u_t \odot h_{t-1} + (1 - u_t) \odot \tilde{h}_t \tag{9}$$

STGCN is trained using the Adam optimizer. The model training goal is to get the predicted value as close to the true value as possible, thus obtaining the loss function of the model training as shown in Equation (10):

$$Loss = \|y_t - \hat{y}_t\| + \lambda L_{reg} \tag{10}$$

where  $L_{reg}$  denotes the L2 regularization, and  $\lambda$  is the hyperparameter controlling the regularization rate.

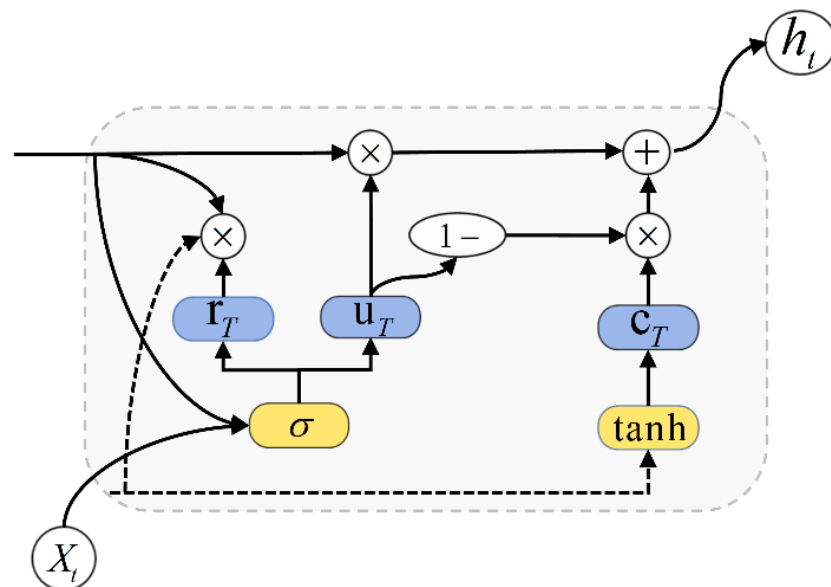


Figure 6. GRU network structure.

## 4. Experiment

### 4.1. Dataset

Thirty sectors in the Shanghai control area were selected for the experiment. The experimental dataset included the adjacency matrix of the 30 sectors, the air traffic situation data of the sectors, and the traffic volume statistics.

- **Adjacency matrix** The Shanghai control area contains 30 sectors. The adjacency matrix was constructed based on whether there was a route connection between the sectors. If there was a route connection between sector  $i$  and sector  $j$ ,  $A_{ij} = 1$ ; otherwise,  $A_{ij} = 0$ . The adjacency matrix  $A \in \mathbb{R}^{30 \times 30}$  was obtained through statistics.
- **Airspace traffic situation data** First, based on the daily traffic volume statistics and flow control information of each sector in Shanghai from 4 August 2018 to 31 October 2018, the free state periods and saturation state periods of each sector were determined. Second, the remaining unmarked periods were used as intermediate states. Third, the sample states of each sector were marked in 15-min time slices. The reason for marking the sector traffic situation in 15-min time slices is that air traffic management departments often use 15-min time slices to measure the sector's operational status and develop and implement traffic control strategies. Furthermore, this paper focuses on the air traffic situation in the sector rather than the operational status changes of specific aircrafts, so a shorter time unit is not chosen. The obtained state dataset of each sector contained a total of 8544 data for 89 days ( $96 \times 89$ ). The data of all sectors were further combined to obtain the feature matrix  $S \in \mathbb{R}^{30 \times 8544}$ .
- **Sector traffic volume data** Based on the radar trajectory data from 4 August 2018 to 31 October 2018, the sector traffic volume information was counted in 15-min time slices. The traffic volume dataset of each sector contained a total of 8544 ( $96 \times 89$ ) data for 89 days, and the dynamic feature matrix  $D \in \mathbb{R}^{30 \times 8544}$  for 30 sectors was obtained.

### 4.2. Parameter Setting

The model was compiled based on TensorFlow. Root-mean-square error (RMSE), mean absolute error (MAE), and accuracy were used as model evaluation metrics. The formulae are shown in Equations (11)–(13), where  $y_t$  denotes the true label value,  $\hat{y}_t$  denotes the predicted value, and  $n$  denotes the number of predicted samples.

$$RMSE = \sqrt{\frac{1}{n} \sum_{i=1}^n (y_t - \hat{y}_t)^2} \quad (11)$$

$$MAE = \frac{1}{n} \sum_{i=1}^n |y_t - \hat{y}_t| \quad (12)$$

$$Accuracy = 1 - \frac{\|y_t - \hat{y}_t\|_F}{\|y\|} \quad (13)$$

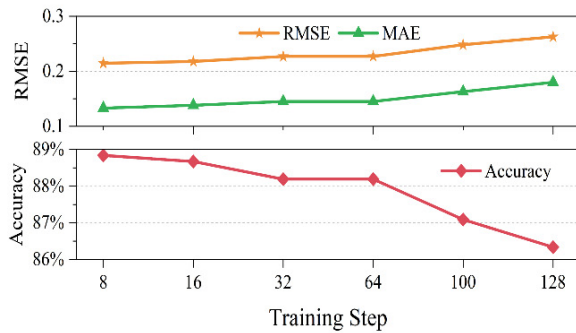
The average precision and recall of each class of samples were used to measure the model's classification performance after the training was completed.  $Precision_i$  and  $Recall_i$  denote the precision and recall of the samples of class  $i$ .  $true\ positive_i$  indicates the case where the model correctly predicts the samples of that class;  $false\ positive_i$  is the case where the model incorrectly predicts the samples of that class; and  $false\ negative_i$  is the case where the samples of that class are predicted as samples of other classes and are incorrectly predicted.

The parameters used in the model training process included learning rate, training set ratio, sequence length, model training step, number of GRU units, and number of model training epochs. The learning rate was set to 0.001, and the training set ratio was set to 0.8. The model training step length, the number of GRU units, and the number of model

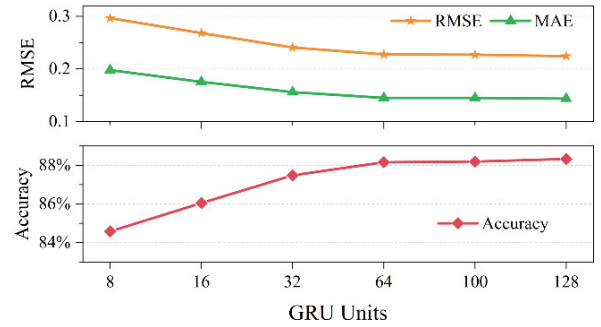
training epochs were determined by parameter experiments and were finally set to 16, 100, and 3000, respectively. The experimental results are shown in Figure 7.

$$Precision_i = \frac{true\ positive_i}{true\ positive_i + false\ positive_i} \quad (14)$$

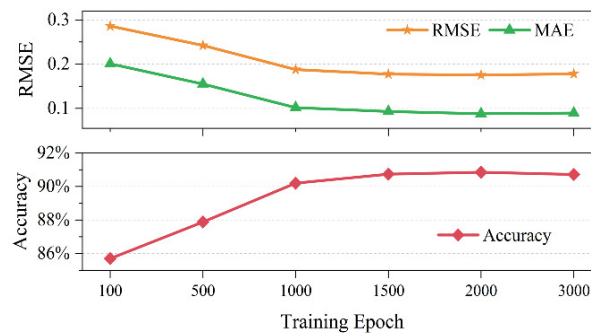
$$Recall_i = \frac{true\ positive_i}{true\ positive_i + false\ negative_i} \quad (15)$$



(a) Parameter experiments for training step



(b) Parameter experiments for GRU units



(c) Parameter experiments for training epoch

**Figure 7.** Parametric experimental results. (a). Effect of different training steps on STGCN performance with 100 GRU units and 500 model training epochs. (b). Effect of the different numbers of GRU units on STGCN performance with 500 training epochs and 16 training steps. (c). Effect of the different number of training epochs on STGCN performance with 100 GRU units and 16 training steps.

Model training was performed using five-fold cross validation. The training and testing data were randomly selected from the total dataset. The data size ratio of the training set to the testing set was 4:1.

The model batch size was set to (8, 16, 32, 64, 100, 128), and the optimal batch size was discovered under the conditions of 100 GRU units and 500 model training epochs. The experimental results are shown in Figure 7a. The experimental results revealed that the model training effect was the best when the model training batch size was 16.

- The range of the number of GRU units is generally chosen as an exponent of 2. The range of the number of GRU units was set to (8, 16, 32, 64, 100, 128) in the experiments of this study. The experimental effects of different numbers of GRU units were tested by fixing the number of model training epochs to 500 and the training step size to 16, as shown in Figure 7b. The experimental results revealed that the model training effect tended to be stable when the number of GRU units was 100; thus, the number of model training GRU units was set to 100.

- The range of model training epochs was set to (500, 1000, 1500, 2000, 3000, 3500). The experimental effect of different training epochs was tested when the training step was 16 and the number of GRU units was 100, and the results are shown in Figure 7c. The experimental results revealed that the model training results tended to be stable when the number of model training rounds reached 3000; thus, the number of model training epochs was set to 3000.

#### 4.3. Experimental Results

The data of 12 historical time slices were used to predict the data of 1–4 future time slices, i.e., the prediction of the future 15/30/45/60 min of the situation characteristics. This section evaluates the prediction effectiveness of the STGCN model along with several benchmark models on the multi-sector air traffic situation based on the following three evaluation metrics: RMSE, MAE, and Accuracy. The benchmark comparison models include the History Average Model (HA), Autoregressive Integrated Moving Average Model (ARIMA), SVR, LSTM, and GRU models. The STGCN-nef model has the same structure as the STGCN model, consisting of a two-layer GCN and a one-layer GRU network; however, the dynamic feature of traffic volume is not incorporated in the model's input. The comparison of the experimental results of the above models is shown in Table 3.

**Table 3.** Comparing the regression prediction performance of different models on the dataset of air traffic situation in 30 Shanghai control sectors.

Prediction Range	Metrics	HA	ARIMA	SVR	LSTM	GRU	STGCN-Nef	STGCN
15-min	RMSE	0.120	1.302	0.257	0.241	0.203	0.185	0.153
	MSE	0.056	1.230	0.191	0.152	0.128	0.099	0.084
	Accuracy	81.20%	27.70%	86.60%	87.50%	89.40%	90.40%	92.00%
30-min	RMSE	0.120	1.301	0.275	0.262	0.241	0.217	0.165
	MSE	0.056	1.229	0.213	0.168	0.159	0.119	0.087
	Accuracy	81.20%	27.80%	85.70%	86.40%	87.50%	88.70%	91.40%
45-min	RMSE	0.120	1.300	0.298	0.282	0.280	0.247	0.168
	MSE	0.056	1.228	0.230	0.193	0.197	0.138	0.085
	Accuracy	81.20%	27.80%	84.40%	85.40%	85.40%	87.10%	91.30%
60-min	RMSE	0.120	1.301	0.313	0.300	0.291	0.265	0.179
	MSE	0.056	1.230	0.243	0.202	0.202	0.150	0.090
	Accuracy	81.20%	27.80%	83.70%	84.40%	84.90%	86.20%	90.70%

Based on the experimental results in Table 3, a comparative analysis was conducted to obtain the following four conclusions:

1. The STGCN model has a high prediction accuracy. The prediction accuracy of the STGCN model for the future 15 min, 30 min, 45 min, and 60 min is above 90%; the prediction accuracy of benchmark models such as HA, SVR, LSTM, and GRU is above 80%; and the prediction accuracy of the ARIMA model is relatively low, i.e., approximately 27%. The experimental results fully demonstrate the predictive advantages of the STGCN model.
2. The STGCN model has an excellent long-term predictive ability. Further analysis of the STGCN model prediction accuracy for the future 15 min, 30 min, 45 min, and 60 min revealed that the model prediction accuracy is the highest when the prediction time step is 15-min (92.00%). The model prediction accuracy decreases slightly when the model prediction time step is 60-min (90.70%). However, the overall model prediction accuracy is above 90%.
3. The STGCN model has excellent spatiotemporal prediction performance. The prediction performance of two benchmark models, LSTM and GRU, were compared with STGCN. The highest prediction accuracies of the LSTM, GRU, and STGCN models

are 87.5%, 89.40%, and 92.00%, respectively. The prediction performance of the GRU model is better than that of the LSTM model; however, the overall prediction accuracy of both the GRU and LSTM models is lower than that of the STGCN model. This indicates that compared with the traditional time series prediction models, the STGCN model effectively learns the spatial structural features between sectors through the GCN to achieve more accurate situation prediction results.

4. The STGCN model effectively improves the model prediction accuracy by merging dynamic features. Comparing the prediction accuracy of the STGCN model and the STGCN-nef model for the future 15 min, 30 min, 45 min, and 60 min changes in the situation revealed that the STGCN model outperforms the STGCN-nef model for multiple time steps. This shows that the STGCN model effectively improves the prediction by merging the dynamic features of traffic volume.

The classification accuracy and recall results of the STGCN model and the baseline model in predicting different time steps are shown in Table 4, in which the classification performance of STGCN outperformed the other five baseline models and STGCN-nef in all four types of time steps. Although the classification precision of STGCN decreased when the prediction step was gradually increased, the overall classification precision and recall remained above 94%, further indicating that STGCN has better prediction precision and long-term prediction ability.

**Table 4.** Comparing the classification performance of different models on the dataset of air traffic situations in 30 Shanghai control sectors.

Prediction Range	Metrics	HA	ARIMA	SVR	LSTM	GRU	STGCN-nef	STGCN
15-min	Precision	80.98%	38.61%	91.82%	95.85%	96.28%	96.32%	97.91%
	Recall	79.17%	49.08%	91.81%	92.75%	94.52%	95.05%	97.71%
30-min	Precision	80.98%	38.53%	90.25%	93.47%	94.06%	94.70%	97.15%
	Recall	79.17%	49.22%	90.22%	90.86%	91.22%	93.64%	96.02%
45-min	Precision	80.98%	38.47%	89.68%	91.38%	93.40%	92.57%	96.64%
	Recall	79.17%	49.51%	89.64%	88.53%	89.81%	91.27%	95.95%
60-min	Precision	80.98%	38.35%	87.09%	90.09%	91.86%	92.15%	95.89%
	Recall	79.17%	49.52%	88.73%	86.77%	87.09%	90.04%	94.33%

## 5. Conclusions

The main contributions of this paper include:

1. Rapid calibration of the air traffic situation using flow control data accurately reflects the controller's workload. Three sector operational states—a free state, saturated state, and intermediate state—were defined by combining traffic statistics and flow control information. This effectively solves the difficulty of obtaining a large number of labeled samples. However, the intermediate state samples are currently not defined with a specific saturation degree. In the future, we will continue to refine the saturation degree of the intermediate state to increase the accuracy of the airspace operation status prediction results.
2. By abstracting the airspace network as an undirected graph, the STGCN is constructed to predict the changing characteristics of the air traffic situation in large-scale airspace. The experimental results in 30 sectors within the Shanghai control area show that the prediction effect of the STGCN model is significantly better than that of the traditional temporal prediction model. It proves that the GCN can effectively capture the interaction relationships between sectors and achieve more accurate situational predictions. In the future, we will continue to refine the construction of a large-scale airspace network and try to abstract it as a directed graph. We will also attempt to introduce an attention mechanism in STGCN to improve its prediction performance.

3. The STGCN model has an average prediction accuracy of more than 90% for the future situation within 1 h, which indicates a good long-term predictive ability. In comparison with other benchmark methods, the STGCN model has significant advantages and can be applied to the prediction of multi-sector airspace operations in large regional control centers.

**Author Contributions:** Conceptualization, D.S.; methodology, Q.L. and K.L.; software, Q.L. and K.L.; validation, K.L.; formal analysis, D.S.; investigation, D.S.; resources, D.S.; data curation, Q.L. and K.L.; writing—original draft preparation, K.L.; writing—review and editing, K.L.; visualization, K.L.; supervision, D.S. and K.L.; project administration, D.S.; funding acquisition, D.S. All authors have read and agreed to the published version of the manuscript.

**Funding:** The research is funded by the Civil Aviation Administration of China (CAAC). The project type is Civil Aviation Safety Capacity Building Project, grant number ([2022] No. 125).

**Data Availability Statement:** Not applicable.

**Conflicts of Interest:** The authors declare no conflict of interest.

## References

1. Delahaye, D.; Puechmorel, S. Air traffic complexity based on dynamical systems. In Proceedings of the 49th IEEE Conference on Decision and Control (CDC), Atlanta, GA, USA, 15–17 December 2010; pp. 2069–2074.
2. Lee, K.; Feron, E.; Pritchett, A. Describing airspace complexity: Airspace response to disturbances. *J. Guid. Control Dyn.* **2009**, *32*, 210–222. [\[CrossRef\]](#)
3. Djokic, J.; Lorenz, B.; Fricke, H. Air traffic control complexity as workload driver. *Transp. Res. Part C Emerg. Technol.* **2010**, *18*, 930–936. [\[CrossRef\]](#)
4. Laudeman, I.V.; Shelden, S.G.; Branstrom, R.; Brasil, C. *Dynamic Density: An Air Traffic Management Metric*; NASA: Washington, DC, USA, 1998.
5. Delahaye, D.; Paimblanc, P.; Puechmorel, S.; Histon, J.; Hansman, R. A new air traffic complexity metric based on dynamical system modelization. In Proceedings of the 21st Digital Avionics Systems Conference, Irvine, CA, USA, 27–31 October 2002; p. 4A2.
6. Gianazza, D. Airspace configuration using air traffic complexity metrics. In Proceedings of the ATM 2007, 7th USA/Europe Air Traffic Management Research and Development Seminar, Barcelona, Spain, 2–5 July 2007; pp. 1–11.
7. Prandini, M.; Putta, V.; Hu, J. A probabilistic measure of air traffic complexity in 3-D airspace. *Int. J. Adapt. Control Signal Process.* **2010**, *24*, 813–829. [\[CrossRef\]](#)
8. Delahaye, D.; Puechmorel, S. Air Traffic Complexity: Towards an Intrinsic Metric. In Proceedings of the 3rd USA/Europe Air Traffic Management R and D Seminar, Napoli, Italy, 13–16 June 2000.
9. Gianazza, D.; Guittet, K. Selection and evaluation of air traffic complexity metrics. In Proceedings of the 2006 IEEE/AIAA 25TH Digital Avionics Systems Conference, Portland, OR, USA, 15–18 October 2006; pp. 1–12.
10. Gianazza, D.; Guittet, K. Evaluation of air traffic complexity metrics using neural networks and sector status. In Proceedings of the 2nd International Conference on Research in Air Transportation, ICRAT, Portland, OR, USA, 15–18 October 2006; pp. 126–136.
11. Xiao, M.; Zhang, J.; Cai, K.; Cao, X. ATCEM: A synthetic model for evaluating air traffic complexity. *J. Adv. Transp.* **2016**, *50*, 315–325. [\[CrossRef\]](#)
12. Zhu, X.; Cai, K.; Cao, X. A semi-supervised learning method for air traffic complexity evaluation. In Proceedings of the 2017 Integrated Communications, Navigation and Surveillance Conference (ICNS), Herndon, VA, USA, 18–20 April 2017; pp. 1A3-1-1A3-11.
13. Cao, X.; Zhu, X.; Tian, Z.; Chen, J.; Wu, D.; Du, W. A knowledge-transfer-based learning framework for airspace operation complexity evaluation. *Transp. Res. Part C Emerg. Technol.* **2018**, *95*, 61–81. [\[CrossRef\]](#)
14. Zhang, Z.; Zhu, X.; Zhu, S.; Zhang, M.; Du, W. Unsupervised evaluation of airspace complexity based on kernel principal component analysis. *Acta Aeronaut. Astronaut. Sin.* **2019**, *8*, 241–247.
15. Liu, H.; Lin, Y.; Chen, Z.; Guo, D.; Zhang, J.; Jing, H. Research on the air traffic flow prediction using a deep learning approach. *IEEE Access* **2019**, *7*, 148019–148030. [\[CrossRef\]](#)
16. Gui, G.; Zhou, Z.; Wang, J.; Liu, F.; Sun, J. Machine learning aided air traffic flow analysis based on aviation big data. *IEEE Trans. Veh. Technol.* **2020**, *69*, 4817–4826. [\[CrossRef\]](#)
17. Bai, J.; Zhu, J.; Song, Y.; Zhao, L.; Hou, Z.; Du, R.; Li, H. A3t-gcn: Attention temporal graph convolutional network for traffic forecasting. *ISPRS Int. J. Geo-Inf.* **2021**, *10*, 485. [\[CrossRef\]](#)
18. Guo, S.; Lin, Y.; Feng, N.; Song, C.; Wan, H. Attention based spatial-temporal graph convolutional networks for traffic flow forecasting. In Proceedings of the AAAI Conference on Artificial Intelligence, Honolulu, HI, USA, 27 January–1 February 2019; pp. 922–929.

19. Li, Y.; Yu, R.; Shahabi, C.; Liu, Y. Diffusion convolutional recurrent neural network: Data-driven traffic forecasting. *arXiv* **2017**, arXiv:1707.01926.
20. Wang, X.; Ma, Y.; Wang, Y.; Jin, W.; Wang, X.; Tang, J.; Jia, C.; Yu, J. Traffic flow prediction via spatial temporal graph neural network. In Proceedings of the Web Conference, Taiwan, China, 20–24 April 2020; pp. 1082–1092.
21. Zhao, L.; Song, Y.; Zhang, C.; Liu, Y.; Wang, P.; Lin, T.; Deng, M.; Li, H. T-gcn: A temporal graph convolutional network for traffic prediction. *IEEE Trans. Intell. Transp. Syst.* **2019**, *21*, 3848–3858. [[CrossRef](#)]
22. Zhu, J.; Wang, Q.; Tao, C.; Deng, H.; Zhao, L.; Li, H. AST-GCN: Attribute-augmented spatiotemporal graph convolutional network for traffic forecasting. *IEEE Access* **2021**, *9*, 35973–35983. [[CrossRef](#)]
23. Bai, L.; Yao, L.; Li, C.; Wang, X.; Wang, C. Adaptive graph convolutional recurrent network for traffic forecasting. *Adv. Neural Inf. Process. Syst.* **2020**, *33*, 17804–17815.
24. Li, F.; Feng, J.; Yan, H.; Jin, G.; Yang, F.; Sun, F.; Jin, D.; Li, Y. *Dynamic Graph Convolutional Recurrent Network for Traffic Prediction: Benchmark and Solution*; Association for Computing Machinery: New York, NY, USA, 2021.
25. Yu, B.; Yin, H.; Zhu, Z. Spatio-temporal graph convolutional networks: A deep learning framework for traffic forecasting. *arXiv* **2017**, arXiv:1709.04875.
26. Wu, Z.; Pan, S.; Long, G.; Jiang, J.; Zhang, C. Graph wavenet for deep spatial-temporal graph modeling. *arXiv* **2019**, arXiv:1906.00121.
27. Song, C.; Lin, Y.; Guo, S.; Wan, H. Spatial-temporal synchronous graph convolutional networks: A new framework for spatial-temporal network data forecasting. In Proceedings of the AAAI Conference on Artificial Intelligence, New York, NY, USA, 7–12 February 2020; pp. 914–921.
28. Li, M.; Zhu, Z. Spatial-temporal fusion graph neural networks for traffic flow forecasting. In Proceedings of the AAAI Conference on Artificial Intelligence, Vancouver, BC, Canada, 2–9 February 2021; pp. 4189–4196.
29. Lin, Y.; Zhang, J.-W.; Liu, H. Deep learning based short-term air traffic flow prediction considering temporal–spatial correlation. *Aerosp. Sci. Technol.* **2019**, *93*, 105113. [[CrossRef](#)]
30. Wu, Z.; Pan, S.; Chen, F.; Long, G.; Zhang, C.; Philip, S.Y. A comprehensive survey on graph neural networks. *IEEE Trans. Neural Netw. Learn. Syst.* **2020**, *32*, 4–24. [[CrossRef](#)] [[PubMed](#)]